The Impact of Human Walking on the Time-Frequency Distribution of In-Home Radio Channels

Alireza Borhani and Matthias Pätzold
Faculty of Engineering and Science, University of Agder, Grimstad, Norway
Emails: {alireza.borhani, matthias.paetzold}@uia.no

***Abstract*—Passive activity recognition of home occupants has become a very hot topic in the area of radio communications, as it enables the development of cutting-edge healthcare monitoring solutions. Thanks to ubiquitous radio waves, such as WiFi signals, at today's homes, one can process radio waves reflected off a person's body for identifying certain mobility patterns. This new approach ignores the need for any wearable sensors. This paper reports a challenging indoor radio channel measurement campaign at 5.9 GHz, which has been conducted to study the impact of walking persons on the temporal and spectral properties of the channel. In particular, the time-frequency distribution of the channel has been investigated by spectrogram analysis. It is shown that the spectrogram not only contains fingerprint information of the walking activity, but also allows for the discrimination of two different walking persons. Similar observations can hardly be made by standard techniques based on the analysis of temporal variations of the received channel envelope. The results presented in the paper are useful for the development of passive activity recognition algorithms.**

I. INTRODUCTION

Worldwide, nearly 3.2 million deaths per year are being attributed to inactivity [1]. Adding the increase of global average life expectancy by 5 years from 2000 and 2015, the levels of chronic health conditions are increasing, and the levels of physical activities are declining. The inactivity of elderlies increases the risk of fall incidents. According to the World Health Organization [1], around one third of people aged 65+ years fall at least twice a year. Such incidents come often with serious physical injuries followed by hikikomori (extreme social isolation), if not kodokushi (long-term undiscovered lonely death). This increases the demand for in-home activity monitoring of elderly people, such that their privacy and comfort do not be affected by, e.g., wearable sensors and/or vision sensors [2].

Such a global demand has triggered a new approach to health surveillance that employs radio waves reflected off the human body to detect user activity without any need for their active involvement. The new approach is indeed a passive indoor radar solution that transmits radio waves throughout the propagation environment, while fingerprints of the user activities on those waves are collected and processed at the receiver. This process can range from measuring the overall physical activity, through counting the number of upward/downward steps, up to detecting irregular activities such as fall incidents [3], [4]. The challenge of the new approach is threefold. Firstly, the channel characteristics must be collected and pre-processed in response to the person's activities. Secondly, sophisticated signal processing techniques must be applied to these characteristics to extract the fingerprint information from user activity. Thirdly, robust detection algorithms must be designed to distinguish similar activities. This paper addresses the first and the second challenges, which have not been sufficiently studied in the literature. In [5], the signal strength data collected from a radio frequency identification (RFID) sensor was employed for activity recognition purposes. An ultra-wide band (UWB) sensor with an operating frequency between 3.1 GHz and 5.6 GHz was used in [6] to detect fall incidents based on the temporal characteristics of the channel. The impact of human activity on the temporal properties of the channel was also studied in [7]. In addition, a more theoretical study on the influence of walking people on the Doppler spectral characteristics of indoor channels can be found in [8]. The WiTrack system employs a multiple antenna frequency modulated carrier wave radar with a total bandwidth of 1.69 GHz to track a person's 3D movements from the radio signals reflected off the body [9]. In this paper, we report an in-home channel measurement campaign performed in a typical Norwegian house using a radio channel sounder operating at 5.9 GHz. To reveal the time-frequency behavior of the channel, a spectrogram analysis has been performed on the channel impulse response (CIR), estimating the Doppler power spectrum in time. It is demonstrated that the spectrogram is imprinted by the walking activity of a moving person. It is shown that the impacts of two different persons on the spectrogram are also visible and distinguishable. Useful information about the trajectory of the performer(s) is also contained into the spectrogram. In contrast, it is shown that the channel envelope does not reveal such detailed information. The remainder of this paper is organized as follows. The radio channel sounder and the experimental setups are introduced in Section II. Section III outlines the theoretical background of the conducted time-frequency analysis, while Section IV illustrates the obtained characteristics and interprets the results. Finally, Section V concludes the paper.

II. MEASUREMENT SETUP

System: A research radio channel sounder developed at the Norwegian University of Science and Technology (NTNU)

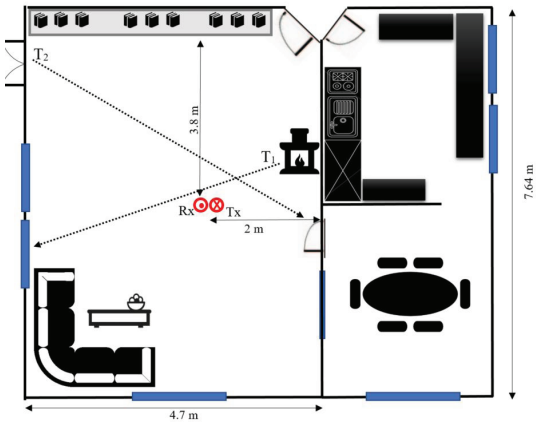

Fig. 1. A schematic presentation of the propagation environment, illustrating Trajectory T_1 and T_2 of the performers, as well as the position (red solid-line circles) of the Tx/Rx antennas.

and owned by Super Radio AS (university spin-off) was used to conduct the measurement campaign. The channel sounder employs the time-division multiplexing technique, operates at 5.9 GHz, and records the time-variant (TV) channel transfer function (CTF). The signal bandwidth is 100 MHz, allowing for a sampling frequency f_s of 200 MHz. Both the transmitter (Tx) and the receiver (Rx) are equipped with single omni-directional antennas. The Tx is configured to transmit 6187 chirps per second, while each chirp contains 512 samples. ***Environment:*** The campaign was conducted in the living room of a typical two-story Norwegian house located in Grimstad, Norway. The foundation of the building is concrete, while the rest of the structure is mainly wood. The living room is on the first floor with an area of about 36 m^2 and a ceiling height of 2.4 m. The room has standard furniture, such as a sofa set, sofa table, fireplace, library, etc. A schematic plot of the measurement setup/environment is shown in Fig. 1. The figure also contains the approximate trajectories T_1 and T_2 of the two users. ***Scenarios:*** The Tx and Rx were located almost in the middle of the room, but at different heights. The Tx was placed on the floor, having a line-of-sight to the Rx mounted on below the ceiling at the height of 2.2 m. The red solid-line circle $\odot$ ($\otimes$) in Fig.1 depicts the position of the Rx (Tx) in the considered setting.

The radio channel measurements for three scenarios were carried out with two actors (P1, P2), both approx. 1.78 m tall. The three scenarios are designed as follows: ***Reference***: P1 and P2 stay out of the living area, where no physical activities take place. This scenario provides a benchmark for comparing the properties of the stationary channel to those of the non-stationary channels. ***Walking 1***: P2 stays out of the living area, while P1 walks slowly along the trajectory T_1 from the fireplace towards the window (see Fig. 1) and stops when he arrives there. ***Walking 2***: P1 and P2 walk slowly along the trajectories T_1 and T_2, respectively, and stop when each of them arrives. The presence of very slow moving scatterers is inevitable. For instance, two system operators and a reporter were also in the room, but they were asked to stay stationary working with their laptops out of the living area.

III. Analysis Methodology

The raw data that the channel sounder measures is the TV CTF $H(f',t)$. The corresponding TV CIR $h(\tau',t)$ can be obtained by taking the inverse Fourier transform of $H(f',t)$ with respect to f'. The TV CIR can be expressed by the following sum $h(\tau',t)=\sum_{n=1}^{N}\mu_n(t)\delta(\tau'-\tau'_n(t))$, in which N is the total number of multipath components, $\mu_n(t)$ represents the TV complex gain of the nth path, $\delta(\cdot)$ denotes the Dirac delta function, and $\tau'_n(t)$ describes the TV propagation delay associated with the nth propagation path. The complex channel gain is $\mu(t)$ is obtained by integrating $h(\tau',t)$ with respect to τ'.

A very practical approach to study the time-frequency distribution of non-stationary channels is to perform a spectrogram analysis on the complex channel gain. This is done by first multiplying $\mu(t')$ with a sliding window function $w(t'-t)$, i.e., $x(t',t)=\mu(t')w(t'-t)$, where $w(t)$ is a positive even function with unit energy, and then applying the Fourier transform to the windowed signal $x(t',t)$ with respect to t', i.e., $X(f,t)=\int_{-\infty}^{\infty}x(t',t)e^{-j2\pi ft'}dt'$. The spectrogram $S_{xx}(f,t)$ is then defined as the squared magnitude of the short-time Fourier transform $X(f,t)$, i.e., $S_{xx}(f,t)=|X(f,t)|^2$, which estimates the power spectral density of the Doppler frequencies in time. Herein, we employ a Gaussian window function $w(t)$, with a window spread parameter set to $\sigma_\omega=50$ ms.

IV. Measurement Results

Fig. 2 illustrates the channel envelope $|\mu(t)|$ and the spectrogram $S_{xx}(f,t)$ of the process $\mu(t)$ corresponding to the Reference scenario and the Walking 1 scenario. Comparing Figs. 2 (a) and (c), it is clear that the variation of the channel in the reference scenario is significantly less than that of the walking scenario. However, explaining the measured channel envelope is not straightforward, as it shows just typical small-scale fading behaviour. In contrast, the spectrogram of the channel contains useful information about the propagation environment and the motion of its elements in time. Fig. 2 (b) shows the spectrogram of the reference scenario, in which the zero frequency components all along the time axis confirms that the propagation area is stationary. The near-zero frequencies are artefact caused by the limited frequency resolution of the spectrogram. Slow movements of operators' hands and even their heartbeat can be another reason for the near-zero frequency components. The spectrogram of the channel associated with the Walking 1 scenario is shown in Fig. 2(d), in which we have filtered out the impact of fixed objects. This plot reveals the mobility pattern of the performer in the following manner. The person starts accelerating from a zero speed to a maximum walking speed (around 1 m/s), while approaching the Tx/Rx. This results in positive Doppler shifts of about 20 Hz at $t=2$ s. As the person keeps walking along T_1 (see Fig. 1), the arriving/departing waves become almost perpendicular to the direction of motion, resulting in near-zero

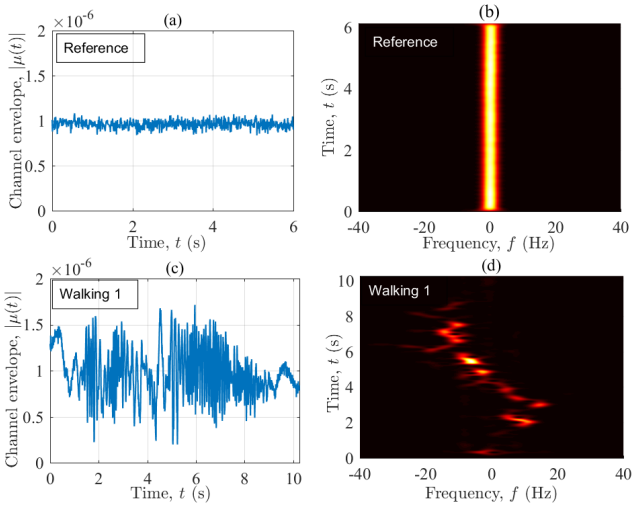

Fig. 2. The channel envelope $|\mu(t)|$ of the (a) Reference and (c) Walking 1 scenarios, as well as the spectrogram $S_{xx}(f,t)$ of the (b) Reference and (d) Walking 1 scenarios.

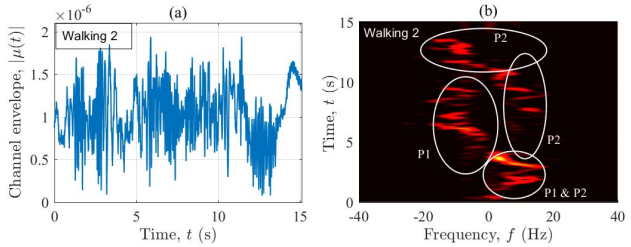

Fig. 3. The channel envelope $|\mu(t)|$ of the (a) Walking 2 scenario, as well as the spectrogram $S_{xx}(f,t)$ of the (b) Walking 2 scenario.

Doppler frequencies at around $t = 5\,\text{s}$. As the person leaves the vicinity of the Tx/Rx, the negative Doppler shifts appear. Finally, the deceleration of P1 to a complete stop at the end of T_1 leads to a zero Doppler shift (already filtered) at about $t = 9\,\text{s}$.

Fig. 2 exhibits the channel envelope $|\mu(t)|$ and the spectrogram $S_{xx}(f,t)$ of the complex channel gain $\mu(t)$ associated with the Walking 2 scenario. Once again, it can be confirmed that the variation of the channel envelope (see Fig. 3 (a)) is considerably larger than that of the Reference scenario (see Fig. 2 (a)). In addition, the ongoing activity can hardly be explained in the illustrated channel envelope. However, the corresponding spectrogram in Fig. 3 (b) reveals the impact of the two moving persons on the time-frequency distribution of the channel. We have marked the contribution of each performer in Fig. 3 (b). The performer P1 walks along T_1 similar to what he did in the Walking 1 scenario. The fingerprints of P1 on the spectrogram shown in Fig. 3 (b) can thus be explained as before (see the interpretation of Fig. 2 (d)). In the Walking 2 scenario, the performer P2 walks along a longer path, i.e., T_2, taking more time to approach the vicinity of the Tx/Rx, where the Doppler shifts are close to zero due to the perpendicularity of the arriving/departing waves. Therefore, for the first 10 s, P2 contributes with positive Doppler shifts as can be observed in Fig. 3 (b). By approaching and then leaving the vicinity of the Tx/Rx, negative Doppler frequencies appear (see $10 < t < 13$ in Fig. 3 (b)). The performer P2 finally stops at the end of T_2, characterized by vanishing Doppler shifts at about $t = 15\,\text{s}$. We remark that cross-terms, as the artefact of the spectrogram analysis, might slightly affect the interpretation of the results.

V. Conclusion

This paper has characterized the time-frequency behaviour of an in-home radio channel using experimental data collected from a measurement campaign at 5.9 GHz. The main goal of the experiment was to study the impact of walking persons on the radio channel characteristics. It is shown that unlike the channel envelope, the spectrogram contains very useful information about the propagation area and its changes due to the walking activity. Moreover, it is shown that the impact of two different walking persons on the channel's time-frequency distribution is distinguishable. It is also shown that the non-stationarity of the channel can hardly be assessed by observing the channel envelope. To better understand the impact of people on the channel characteristics, more channel measurement campaigns at other frequency bands are required.

References

[1] Department of Ageing and Life Course, "WHO global report on falls prevention in older age," 2007.

[2] Z. Zhang, C. Conly, and V. Athitsos, "A survey on vision-based fall detection," in *Proceedings of the 8th ACM Int. Conf. on PErvasive Technologies Related to Assistive Environments*, New York, NY, USA, 2015, PETRA'15, pp. 46:1–46:7, ACM.

[3] B. Erol and M. G. Amin, "Fall motion detection using combined range and Doppler features," in *2016 24th European Signal Processing Conference (EUSIPCO)*, Aug. 2016, pp. 2075–2080.

[4] B. Erol, M. G. Amin, and B. Boashash, "Range-Doppler radar sensor fusion for fall detection," in *2017 IEEE Radar Conference (RadarConf)*, May 2017, pp. 0819–0824.

[5] L. Yao, Q. Z. Sheng, X. Li, T. Gu, M. Tan, X. Wang, and W. Zou, "Compressive representation for device-free activity recognition with passive RFID signal strength," *IEEE Transactions on Mobile Computing*, vol. 17, no. 2, Feb. 2018.

[6] G. Mokhtari, Q. Zhang, and A. Fazlollahi, "Non-wearable UWB sensor to detect falls in smart home environment," in *2017 IEEE International Conference on Pervasive Computing and Communications Workshops (PerCom Workshops)*, Mar. 2017, pp. 274–278.

[7] F. Firoozi, A. Borhani, and M. Pätzold, "Experimental characterization of mobile fading channels aiming the design of non-wearable fall detection radio systems at 5.9 GHz," in *2016 IEEE International Conference on Communication Systems (ICCS)*, Dec. 2016, pp. 1–6.

[8] A. Abdelgawwad and M. Pätzold, "On the influence of walking people on the Doppler spectral characteristics of indoor channels," in *Personal Indoor and Mobile Radio Communications (PIMRC)*. Oct. 2017, Montreal, Canada.

[9] F. Adib, Z. Kabelac, D. Katabi, and R. C. Miller, "3D tracking via body radio reflections," in *14th USENIX Symposium on Networked Systems Design and Implementation*. Apr. 2014, Seattle, USA.